Study of Gluon versus Quark Fragmentation in $\Upsilon \to gg\gamma$ and $e^+e^- \to q\bar{q}\gamma$ Events at $\sqrt{s}=10$ GeV

Abstract

Using data collected with the CLEO II detector at the Cornell Electron Storage Ring, we determine the ratio R_{chrg} for the mean charged multiplicity observed in $\Upsilon(1\mathrm{S}) \to gg\gamma$ events, $< n^{\pm}_{\mathrm{gluon}} >$, to the mean charged multiplicity observed in $e^+e^- \to q\bar{q}\gamma$ events, $< n^{\pm}_{\mathrm{quark}} >$. We find $R_{\mathrm{chrg}} \equiv \frac{<n^{\pm}_{gluon}>}{<n^{\pm}_{\mathrm{quark}}>} = 1.04 \pm 0.02(\mathrm{stat}) \pm 0.05(\mathrm{syst})$ for jet-jet masses less than 7 GeV.

Submitted to Physical Review D

M. S. Alam,[1] S. B. Athar,[1] Z. Ling,[1] A. H. Mahmood,[1] H. Severini,[1] S. Timm,[1]
F. Wappler,[1] A. Anastassov,[2] S. Blinov,[2,1] J. E. Duboscq,[2] D. Fujino,[2,2] R. Fulton,[2]
K. K. Gan,[2] T. Hart,[2] K. Honscheid,[2] H. Kagan,[2] R. Kass,[2] J. Lee,[2] M. B. Spencer,[2]
M. Sung,[2] A. Undrus,[2,1] R. Wanke,[2] A. Wolf,[2] M. M. Zoeller,[2] B. Nemati,[3] S. J. Richichi,[3]
W. R. Ross,[3] P. Skubic,[3] M. Wood,[3] M. Bishai,[4] J. Fast,[4] E. Gerndt,[4] J. W. Hinson,[4]
N. Menon,[4] D. H. Miller,[4] E. I. Shibata,[4] I. P. J. Shipsey,[4] M. Yurko,[4] L. Gibbons,[5]
S. D. Johnson,[5] Y. Kwon,[5] S. Roberts,[5] E. H. Thorndike,[5] C. P. Jessop,[6] K. Lingel,[6]
H. Marsiske,[6] M. L. Perl,[6] S. F. Schaffner,[6] D. Ugolini,[6] R. Wang,[6] X. Zhou,[6] T. E. Coan,[7]
V. Fadeyev,[7] I. Korolkov,[7] Y. Maravin,[7] I. Narsky,[7] V. Shelkov,[7] J. Staeck,[7]
R. Stroynowski,[7] I. Volobouev,[7] J. Ye,[7] M. Artuso,[8] A. Efimov,[8] F. Frasconi,[8] M. Gao,[8]
M. Goldberg,[8] D. He,[8] S. Kopp,[8] G. C. Moneti,[8] R. Mountain,[8] Y. Mukhin,[8] S. Schuh,[8]
T. Skwarnicki,[8] S. Stone,[8] G. Viehhauser,[8] X. Xing,[8] J. Bartelt,[9] S. E. Csorna,[9] V. Jain,[9]
S. Marka,[9] A. Freyberger,[10] D. Gibaut,[10] R. Godang,[10] K. Kinoshita,[10] I. C. Lai,[10]
P. Pomianowski,[10] S. Schrenk,[10] G. Bonvicini,[11] D. Cinabro,[11] R. Greene,[11] L. P. Perera,[11]
B. Barish,[12] M. Chadha,[12] S. Chan,[12] G. Eigen,[12] J. S. Miller,[12] C. O'Grady,[12]
M. Schmidtler,[12] J. Urheim,[12] A. J. Weinstein,[12] F. Würthwein,[12] D. M. Asner,[13]
D. W. Bliss,[13] W. S. Brower,[13] G. Masek,[13] H. P. Paar,[13] M. Sivertz,[13] J. Gronberg,[14]
R. Kutschke,[14] D. J. Lange,[14] S. Menary,[14] R. J. Morrison,[14] S. Nakanishi,[14]
H. N. Nelson,[14] T. K. Nelson,[14] C. Qiao,[14] J. D. Richman,[14] D. Roberts,[14] A. Ryd,[14]
H. Tajima,[14] M. S. Witherell,[14] R. Balest,[15] B. H. Behrens,[15] K. Cho,[15] W. T. Ford,[15]
H. Park,[15] P. Rankin,[15] J. Roy,[15] J. G. Smith,[15] J. P. Alexander,[16] C. Bebek,[16]
B. E. Berger,[16] K. Berkelman,[16] K. Bloom,[16] D. G. Cassel,[16] H. A. Cho,[16]
D. M. Coffman,[16] D. S. Crowcroft,[16] M. Dickson,[16] P. S. Drell,[16] K. M. Ecklund,[16]
R. Ehrlich,[16] R. Elia,[16] A. D. Foland,[16] P. Gaidarev,[16] R. S. Galik,[16] B. Gittelman,[16]
S. W. Gray,[16] D. L. Hartill,[16] B. K. Heltsley,[16] P. I. Hopman,[16] S. L. Jones,[16]
J. Kandaswamy,[16] N. Katayama,[16] P. C. Kim,[16] D. L. Kreinick,[16] T. Lee,[16] Y. Liu,[16]
G. S. Ludwig,[16] J. Masui,[16] J. Mevissen,[16] N. B. Mistry,[16] C. R. Ng,[16] E. Nordberg,[16]
M. Ogg,[16,3] J. R. Patterson,[16] D. Peterson,[16] D. Riley,[16] A. Soffer,[16] C. Ward,[16]
M. Athanas,[17] P. Avery,[17] C. D. Jones,[17] M. Lohner,[17] C. Prescott,[17] S. Yang,[17] J. Yelton,[17]
J. Zheng,[17] G. Brandenburg,[18] R. A. Briere,[18] Y.S. Gao,[18] D. Y.-J. Kim,[18] R. Wilson,[18]
H. Yamamoto,[18] T. E. Browder,[19] F. Li,[19] Y. Li,[19] J. L. Rodriguez,[19] T. Bergfeld,[20]
B. I. Eisenstein,[20] J. Ernst,[20] G. E. Gladding,[20] G. D. Gollin,[20] R. M. Hans,[20] E. Johnson,[20]
I. Karliner,[20] M. A. Marsh,[20] M. Palmer,[20] M. Selen,[20] J. J. Thaler,[20] K. W. Edwards,[21]
A. Bellerive,[22] R. Janicek,[22] D. B. MacFarlane,[22] K. W. McLean,[22] P. M. Patel,[22]
A. J. Sadoff,[23] R. Ammar,[24] P. Baringer,[24] A. Bean,[24] D. Besson,[24] D. Coppage,[24]
C. Darling,[24] R. Davis,[24] N. Hancock,[24] S. Kotov,[24] I. Kravchenko,[24] N. Kwak,[24]
S. Anderson,[25] Y. Kubota,[25] M. Lattery,[25] J. J. O'Neill,[25] S. Patton,[25] R. Poling,[25]
T. Riehle,[25] V. Savinov,[25] and A. Smith[25]

---

[1]Permanent address: BINP, RU-630090 Novosibirsk, Russia.

[2]Permanent address: Lawrence Livermore National Laboratory, Livermore, CA 94551.

[3]Permanent address: University of Texas, Austin TX 78712

[1]State University of New York at Albany, Albany, New York 12222
[2]Ohio State University, Columbus, Ohio 43210
[3]University of Oklahoma, Norman, Oklahoma 73019
[4]Purdue University, West Lafayette, Indiana 47907
[5]University of Rochester, Rochester, New York 14627
[6]Stanford Linear Accelerator Center, Stanford University, Stanford, California 94309
[7]Southern Methodist University, Dallas, Texas 75275
[8]Syracuse University, Syracuse, New York 13244
[9]Vanderbilt University, Nashville, Tennessee 37235
[10]Virginia Polytechnic Institute and State University, Blacksburg, Virginia 24061
[11]Wayne State University, Detroit, Michigan 48202
[12]California Institute of Technology, Pasadena, California 91125
[13]University of California, San Diego, La Jolla, California 92093
[14]University of California, Santa Barbara, California 93106
[15]University of Colorado, Boulder, Colorado 80309-0390
[16]Cornell University, Ithaca, New York 14853
[17]University of Florida, Gainesville, Florida 32611
[18]Harvard University, Cambridge, Massachusetts 02138
[19]University of Hawaii at Manoa, Honolulu, Hawaii 96822
[20]University of Illinois, Champaign-Urbana, Illinois 61801
[21]Carleton University and the Institute of Particle Physics, Ottawa, Ontario, Canada K1S 5B6
[22]McGill University and the Institute of Particle Physics, Montréal, Québec, Canada H3A 2T8
[23]Ithaca College, Ithaca, New York 14850
[24]University of Kansas, Lawrence, Kansas 66045
[25]University of Minnesota, Minneapolis, Minnesota 55455

I. INTRODUCTION

Understanding hadronization, or the process by which elementary partons (gluons and quarks) evolve into mesons and baryons, is complicated by its intrinsically non-perturbative nature. Naively, one expects that because of the greater color charge of gluons compared to quarks, radiation of secondary and tertiary gluons is more likely when hadronization is initiated by a gluon rather than a quark. This results in a greater number of final state hadrons as well as a larger average opening angle between the hadrons in the former case compared to the latter case. In the limit $Q^2 \to \infty$, the ratio of the number of hadrons produced in gluon-initiated jets to the number of hadrons produced in quark-initiated jets is expected, in lowest order, to approach the color degeneracy factor of 9/4 [1].

Many experiments have searched for, and found, multiplicity and jet shape differences between quark and gluon fragmentation [2]- [22]. At Z^0 energies, $q\bar{q}g$ events are readily distinguished by their three-jet topology. Within such events, quark and gluon jets can be separated by a variety of techniques including vertex tagging. Because gluons rarely fragment into heavy quarks, they will produce jets that form a vertex at the e^+e^- interaction point. Quark jets, to the contrary, tend to form a detached vertex when the jet contains a long-lived bottom or charm quark. Unfortunately, the assignment of final state hadrons to the initial state partons is rarely unambiguous and relies on Monte Carlo simulations to determine the fraction of times that an observed hadron is correctly traced to a primary parton.

The 10 GeV center of mass energy range offers a unique opportunity to probe quark and gluon fragmentation effects, without relying on Monte Carlo simulation to associate the final state hadrons with an initial state parton. The decay $\Upsilon(1S) \to gg\gamma$ allows one to compare the gg system in a $gg\gamma$ event with the $q\bar{q}$ system in $e^+e^- \to q\bar{q}\gamma$ events. In both cases, the system recoiling against the photon consists (to lowest order) of hadrons that have evolved from either a two-gluon or a quark-antiquark system. The properties of the recoil systems can then be compared directly.[1]

II. DETECTOR AND DATA SAMPLE

The CLEO II detector [23] is a general purpose solenoidal magnet spectrometer and calorimeter. The detector was designed for efficient triggering and reconstruction of two-photon, tau-pair, and hadronic events. Measurements of charged particle momenta are made with three nested coaxial drift chambers consisting of 6, 10, and 51 layers, respectively. These chambers fill the volume from $r=3$ cm to $r=1$ m, with r the radial coordinate relative to the beam (z) axis. This system is very efficient ($\epsilon \geq 98\%$) for detecting tracks that have transverse momenta (p_T) relative to the beam axis greater than 200 MeV/c, and that are contained within the good fiducial volume of the drift chamber ($|cos\theta|$ <0.94, with θ defined as the

---

[1]Although there may be gluon radiation from the initial partons, we do not distinguish such radiation explicitly in this analysis. Thus, the states that we are comparing are, strictly speaking, $gg\gamma$ and $q\bar{q}\gamma$ to lowest-order only; additional gluon radiation, to which we are not experimentally sensitive, may be present in many of the events in our sample.

polar angle relative to the beam axis). Below this threshold, the charged particle detection efficiency in the fiducial volume decreases to approximately 90% at $p_T \sim$100 MeV/c. For $p_T <$100 MeV/c, the efficiency decreases roughly linearly to zero at a threshold of $p_T \approx$30 MeV/c.

Beyond the time of flight system is the electromagnetic calorimeter, consisting of 7800 thallium doped CsI crystals. The central "barrel" region of the calorimeter covers about 75% of the solid angle and has an energy resolution of

$$\frac{\sigma_{\mathrm{E}}}{E}(\%) = \frac{0.35}{E^{0.75}} + 1.9 - 0.1E; \tag{1}$$

E is the shower energy in GeV. This parameterization translates to an energy resolution of about 4% at 100 MeV and 1.2% at 5 GeV. Two end-cap regions of the crystal calorimeter extend solid angle coverage to about 95% of 4π, although energy resolution is not as good as that of the barrel region. The tracking system, time of flight counters, and calorimeter are all contained within a 1.5 Tesla superconducting coil. Flux return and tracking chambers used for muon detection are located immediately outside the coil and in the two end-cap regions.

We use 63 pb^{-1} of data collected at the Υ(1S) resonance ($\sqrt{s}$=9.46 GeV) as a source of $gg\gamma$ events and 198 pb^{-1} at $\sqrt{s}$=10.52 GeV (on the continuum just below the Υ(4S) resonance) as a source of $q\bar{q}\gamma$ events. The γ in our $q\bar{q}\gamma$ sample results primarily from initial state radiation (ISR) [24]. We compare events for which the invariant masses of the gg and q$\bar{q}$ systems recoiling against the hard photon (M_{recoil}, defined by $M_{recoil} = \sqrt{4E_{\mathrm{beam}}^2(1 - E_\gamma/E_{\mathrm{beam}})}$) are the same.

To suppress low-multiplicity QED events, we require that the thrust of the event (calculated using all the photon candidates and good quality charged tracks) be less than 0.97, and that there be at least 3 good charged tracks in the event. Photon candidates are selected from showers with widths and patterns of energy deposition consistent with that of a photon, as opposed to neutral hadrons (e.g. merged π^0's, K_{L}^0, neutrons, etc.). Owing to the excellent ability of the CLEO-II detector to distinguish high-energy π^0's from photons, approximately 75% of the potential π^0 background is removed at this stage by shower topology cuts. Additional π^0 suppression is achieved with an explicit $\pi^0 \to \gamma\gamma$ mass cut, to be discussed later. To ensure that the events are well-contained within the CLEO detector, we require $|\cos\theta_\gamma| < 0.75$ (θ_γ is defined as before as the polar angle between the beam axis and the direct photon).

In addition to the $gg\gamma$ and $q\bar{q}\gamma$ samples, we search for Υ(1S)$\to ggg$ and $e^+e^- \to q\bar{q}$ events containing a π^0 of energy comparable to the photon in the gamma-tagged sample. These samples, referred to as $gg(\pi^0)$ and $q\bar{q}(\pi^0)$ are used to quantify the background levels from π^0 decays.

III. EXPERIMENTAL TECHNIQUE

One of the most basic parameters used to characterize any event is the mean charged track multiplicity, $< N_{chrg} >$. We plot $< N_{chrg} >$ as a function of the mass recoiling against the direct photon, covering the recoil mass range from 4 to 7 GeV. This mass interval

corresponds to $0.45 < E_\gamma/E_{\text{beam}} < 0.82$ for the $gg\gamma$ sample. We require the recoil mass to be greater than 4 GeV to ensure that we are significantly above the $c\bar{c}\gamma$ threshold; we expect that our $q\bar{q}$ jet sample therefore includes u,d,s,c quarks approximately uniformly, apart from small phase space effects.[2]

To determine the characteristics of $gg\gamma$ events, we must subtract the background from non-resonant $q\bar{q}\gamma$ and $e^+e^- \to \tau\tau\gamma$ events produced in e^+e^- annihilations at $\sqrt{s} = M_{\Upsilon 1S}$. This can be done by direct scaling of the event sample collected at the continuum of the $\Upsilon(4S)$ resonance. In addition to $q\bar{q}\gamma$ events, this latter sample of events also includes $\tau\tau\gamma$ events, as well as any other continuum backgrounds which may be present in our resonant sample. By subtracting this "raw" sample from our $\Upsilon(1S)$ sample, we therefore account for all of the non-resonant backgrounds to $gg\gamma$ at the $\Upsilon(1S)$ energy. We find that before subtraction, this background to $gg\gamma$ comprises about 10% of the gamma-tagged sample taken at the $\Upsilon(1S)$ energy.

Similarly, in order to isolate $q\bar{q}\gamma$ events at 10.52 GeV, we must quantify $\tau\tau\gamma$ contamination. This is done using a Monte Carlo simulation of tau pair events. We find that $\tau\tau\gamma$ events comprise about 10% of the $q\bar{q}\gamma$ data sample passing the other event selection cuts specified above. Beam gas and two photon backgrounds were investigated and found to be negligibly small.

To determine the level of $gg(\pi^0)$ contamination to $gg\gamma$ and $q\bar{q}(\pi^0)$ contamination to $q\bar{q}\gamma$, we first determine how often a single high energy photon can be matched with other photons in the same event to form a π^0. Such photons are explicitly vetoed as likely π^0 daughters. The π^0 contamination, of course, results from cases for which we find only one of the two π^0 daughter photons in the detector [25]. From Monte Carlo simulations, we determine the probability that the second π^0 daughter photon will be found. The likelihood of detecting the second photon varies from 50% at $M_{recoil} = 6.5$ GeV to 77% at $M_{recoil} = 4$ GeV. Knowing the fraction of times that the second daughter photon goes undetected, and the total number of π^0's that we reconstruct in our sample, we thereby determine the fraction of our direct photon candidates which are actually π^0 daughters, but are not vetoed as such. This is shown in (Figure 1) as a function of recoil mass.

Our backgrounds are summarized below:

Sample	$\sqrt{s}$	Background (%)
$gg\gamma$	9.46 GeV	Sum of all non-$\Upsilon(1S)$ events (10%)
$gg\gamma$		$\Upsilon(1S) \to gg(\pi^0)$ contamination to $\Upsilon(1S) \to gg\gamma$ ($\sim 5\%$)
$q\bar{q}\gamma$	10.52 GeV	$\tau\tau\gamma$ (10%)
$q\bar{q}\gamma$		$e^+e^- \to q\bar{q}(\pi^0)$ contamination to $q\bar{q}\gamma$ ($\sim 8\%$)
$q\bar{q}\gamma$		$\gamma\gamma$ ($< 1\%$)
$q\bar{q}\gamma$		beam-gas ($< 1\%$)

[2]We note that the $q\bar{q}$ mixture in our $q\bar{q}\gamma$ sample may be different for cases in which the photon is emitted in the final state as opposed to the initial state due to the different diagrams responsible for these processes. We expect our sample to be dominated by ISR events, as is evidenced by the photon polar angle distribution.

FIG. 1. π^0 contamination, as a function of recoil mass, in $gg\gamma$ events (squares), and in $q\bar{q}\gamma$ events (circles); the y axis gives the fraction of our apparent $gg\gamma$ (or $q\bar{q}\gamma$) event sample which are actually $gg(\pi^0)$ (or $q\bar{q}(\pi^0)$) events.

To determine how our measured charged multiplicity values are biased by the π^0 background, we make a comparison plot of the charged multiplicity distribution for $gg\gamma$ vs. $gg(\pi^0)$ events, and a similar plot for $q\bar{q}\gamma$ vs. $q\bar{q}(\pi^0)$ events. From Figure 2, we see that the charged multiplicity distributions for the gamma-tagged and the π^0-tagged samples are similar.[3] Quantitatively, the effect of π^0 backgrounds is to reduce the measured value of R_{chrg} by about 1% relative to the true value. We statistically correct for this effect in subsequent plots, and include the uncertainty due to π^0 backgrounds in our overall systematic error.

In Figure 3, we show the multiplicity distributions in bins of recoil mass for our background-corrected $gg\gamma$ and $q\bar{q}\gamma$ samples. From the distributions in this Figure, we extract the mean multiplicities as a function of gg or $q\bar{q}$ mass, for pure $gg\gamma$ and $q\bar{q}\gamma$ samples. As shown in Figure 4, the ratio of $< N_{chrg} >$ resulting from gluon fragmentation to $< N_{chrg} >$ from quark fragmentation is $R_{chrg} = 1.04 \pm 0.02$, after all the aforementioned background corrections.

IV. SYSTEMATIC ERRORS

In order to investigate the sensitivity of the result to the $N_{chrg} \geq 3$ requirement and to suppress $\tau\tau\gamma$ backgrounds, we compare the ratios obtained from $N_{chrg} \geq 3$ with ratios obtained using the tightened multiplicity interval $5\leq N_{chrg} \leq 11$. This comparison also partially addresses possible biases in our measured ratio due to acceptance effects as well as the effect of the minimum charged multiplicity cut. If the shapes of the true charged multiplicity distributions were much different for quarks vs. gluons at low multiplicities (for which our acceptance is worse than at high multiplicity, due to the effect of our hadronic event selection cuts as well as trigger effects), then our derived average will be artificially 'pulled' by our $N_{chrg} \geq 3$ requirement. A complete Monte Carlo simulation study of possible differences between the detector level multiplicities and the true multiplicities, including unfolding effects, indicates negligible bias. The value of the ratio using $N_{chrg} > 5$ is found to be statistically consistent with that for $N_{chrg} > 3$. The effect of imposition of the minimum N_{chrg} cut has also been checked by repeating the entire analysis, but using the neutral multiplicity N_{neut} rather than the charged multiplicity as the comparison variable. For this cross-check, we retain the cut $N_{chrg} \geq 3$, but make no cut on the minimum neutral multiplicity. Before any consideration of backgrounds, this cross-check yields $R_{neut} = 1.06 \pm 0.03$ (statistical error only). This value is in good agreement with our measured value of R_{chrg}.

Although we compare systems of equivalent mass, the energies of the systems recoiling against the photon are higher for $q\bar{q}$ events than for gg events at an equivalent invariant mass. On average, the $q\bar{q}\gamma$ system will therefore be more collimated. We investigate possible energy dependent effects with Monte Carlo simulation, by looking at systems of equal recoil mass, but generated at different energies ($\sqrt{s}$=10.52 GeV vs. $\sqrt{s}$=9.46 GeV). We find a

---

[3]It is of some interest to note the similarity in multiplicity between the $gg\gamma$ and the $gg(\pi^0)$ samples. Although the first process contains two primary gluons, whereas the second contains three primary gluons, this plot qualitatively suggests that at these energy scales the available energy for fragmentation is the main factor in determining the final state charged multiplicity.
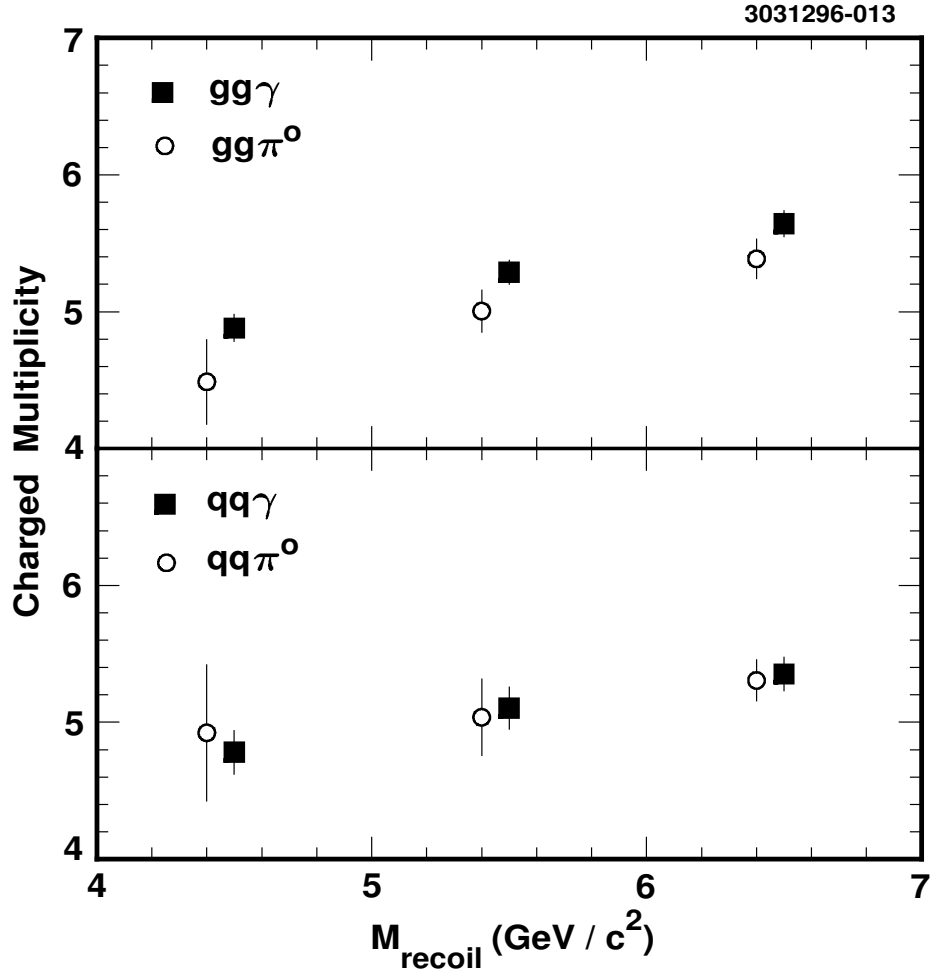
FIG. 2. A comparison of the charged multiplicity distributions for $gg\gamma$ and $gg(\pi^0)$ (top) and $q\bar{q}\gamma$ and $q\bar{q}(\pi^0)$ (bottom).
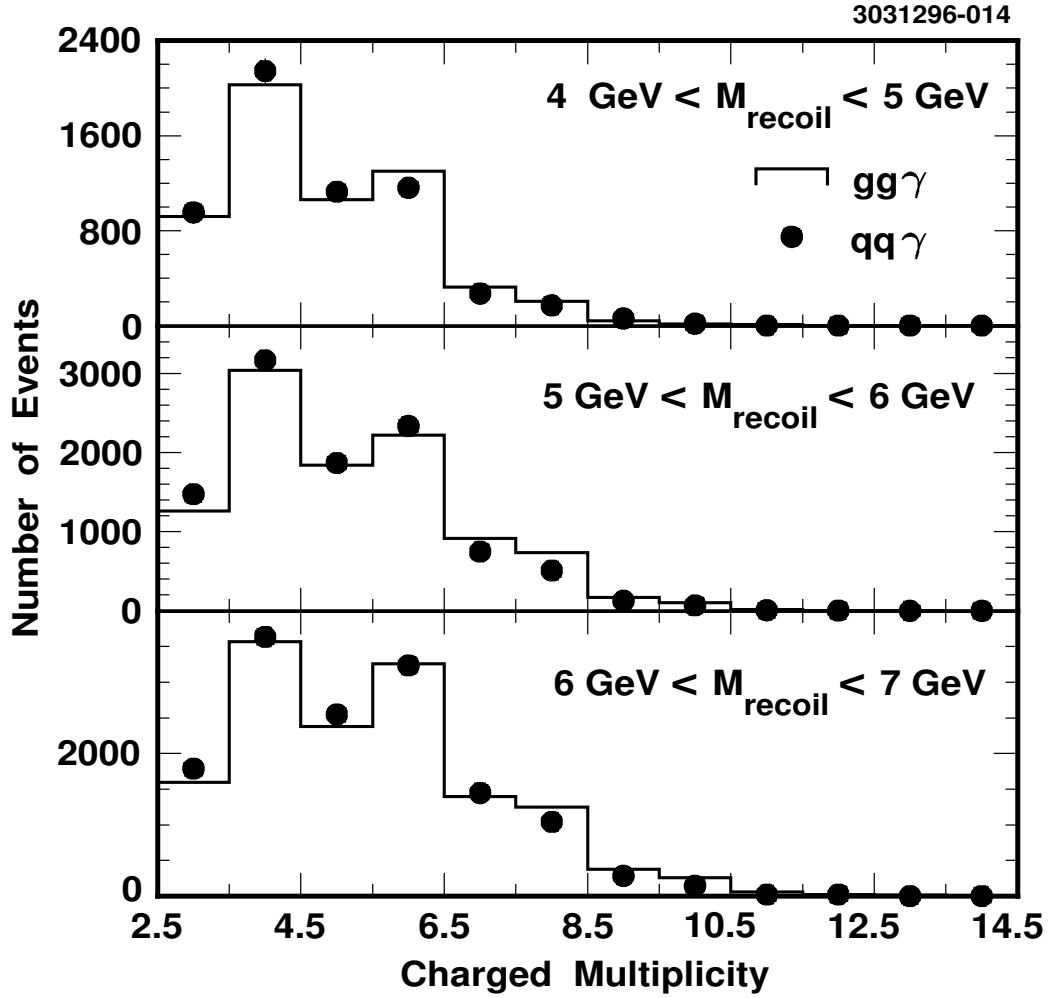
FIG. 3. Observed multiplicity distributions for background subtracted $gg\gamma$ and $q\bar{q}\gamma$ data for different recoil mass ranges.
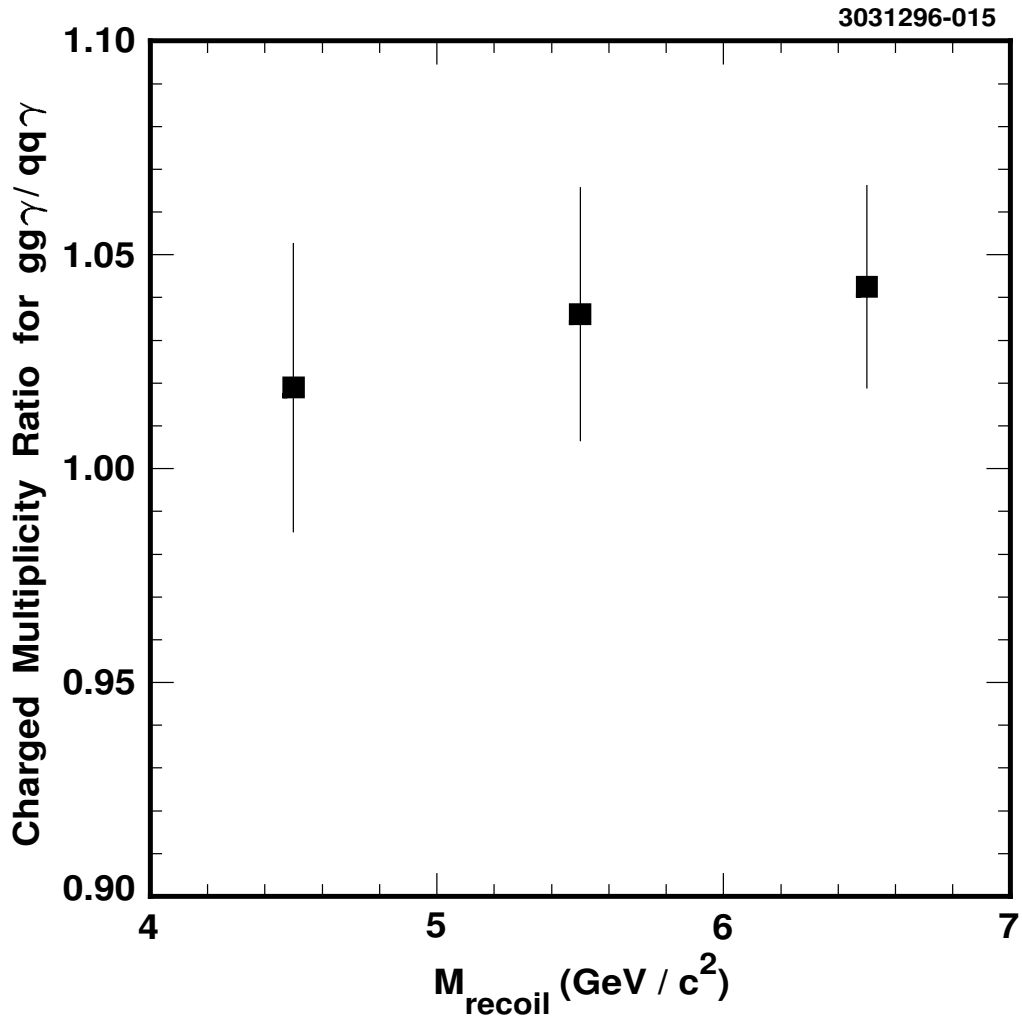
FIG. 4. Charged multiplicity ratio for background subtracted $gg\gamma/q\bar{q}\gamma$ data.

11

systematic shift of 0.006 in the ratios. We can also evaluate energy effects by direct inspection of Figure 4. Although the R_{chrg} values measured for the lowest recoil mass are statistically consistent with the R_{chrg} values measured for the highest recoil mass considered, our results are also consistent with R_{chrg} increasing slightly with recoil mass. We conservatively include a systematic error of 2% to account for any possible systematic variation.

We also compare the $gg\gamma/q\bar{q}\gamma$ multiplicity ratios from data taken during three distinct running periods, covering different running conditions and triggers. The separate data sets give ratios which are all statistically consistent with each other. Nevertheless, we conservatively include the maximum variation of 2% observed between the three data sets in the overall systematic error.

Finally, we consider the dependence of the mean multiplicity on the dip angle, $|\cos\theta_\gamma|$, of the direct photon. We expect that initial state radiation $q\bar{q}\gamma$ events tend to produce photons that are more forward peaked (have larger values of $|\cos\theta_\gamma|$) than for $gg\gamma$. For $q\bar{q}\gamma$ events, we therefore expect that the particles emerging on the other side of the event, opposite the high energy γ, are more likely to be lost down the beam pipe. We have therefore explicitly considered any possible dependence of R_{chrg} on $|cos\theta_\gamma|$ by plotting R_{chrg} in different bins of $|\cos\theta_\gamma|$. At our level of statistical precision, we do not observe any such systematic effect and conclude that the measured R_{chrg} value is not measurably biased by such acceptance effects.[4] We explicitly quantify this by measuring R_{chrg} in two regions of $cos\theta_\gamma$: $|cos\theta_\gamma| < 0.35$, and $0.35 < |cos\theta_\gamma| < 0.70$. The variation between the two ratios is found to be 0.02 ± 0.03. We conservatively assign the error on this value as a measure of the maximum possible systematic error due to such polar angle acceptance effects.

In summary, the systematic errors are:

Systematic Error	Value
π^0 background	0.003
Recoil mass-dependent effects	0.006
Truncated ($5 \leq N_{chrg} \leq 11$) vs. non-truncated mean	0.02
Variation between data sets	0.02
R_{chrg} dependence on M_{recoil}	0.02
$|\cos\theta|$ cut dependence	0.03
Total	0.05

V. SUMMARY

The ratio of $<N_{chrg}>$ for gluons to $<N_{chrg}>$ for quarks measured here is smaller than those found by the OPAL, ALEPH, SLD and DELPHI experiments, at $\sqrt{s} \sim M_{Z^0}$. The

---

[4]There are potentially two competing effects here - although the photon is more forward peaked for $q\bar{q}\gamma$ events, it is also the case that quark jets should be more narrowly collimated than $gg\gamma$ events. This may tend to mitigate any effects due to the difference in photon angular distributions, since charged hadrons produced in $q\bar{q}\gamma$ events should be more contained within the fiducial region of our drift chamber.

ratios compare as follows:

Collaboration	$<N>_g \ / \ <N>_q$	Kinematic Regime
CLEO 96	1.04 ± 0.05	$< E_{jet} > \ \ < \ 7$ GeV
DELPHI [3]	1.24 ± 0.015	$< E_{jet} > = 10\text{-}40$ GeV
DELPHI [3]	1.06 ± 0.18	$< E_{jet} > = 10$ GeV
SLD [16]	1.36 ± 0.24	$< E_{jet} > = 24$ GeV
OPAL 93 [18]	1.27 ± 0.04	$< E_{jet} > = 24$ GeV
ALEPH [20]	1.19 ± 0.04	$< E_{jet} > = 24$ GeV
OPAL 96 [21]*	1.58 ± 0.03	$< E_{jet} > = 39$ GeV

*This OPAL result is for $< N >_g -1/ < N >_q -1$, considering only *uds* quarks

Fuster and Martí [2], DELPHI [3] and Fodor [4] have recently considered how the ratio of charged multiplicity for gluon to quark jets depends on the hadronic center-of-mass energy. Phenomenologically, as the energy scale increases, the likelihood of successive partons radiating also increases. Having a greater color degeneracy than quarks, the multiplicity of gluon-initiated jets increases faster than the multiplicity of quark-initiated jets. This causes R_{chrg} to increase slowly with energy. Our result is smaller than the LEP results for R_{chrg}, showing the expected energy dependence [26]. Our result is also consistent with the measurement by DELPHI at $\sqrt{s} \sim 10$ GeV, albeit with substantially better precision. We note that the $q\bar{q}$ mixture in this experiment is likely to be different than the quark mixture for the high energy experiments mentioned above. Recent analyses by OPAL [22] and ALEPH [20], in fact, have explicitly measured the difference in ratio values when comparing gluon jets to b-quark jets versus gluon jets to uds-quark jets.

VI. ACKNOWLEDGMENTS

REFERENCES

[1] S. J. Brodsky and J. Gunion, *Phys. Rev. Lett. 37*, 402 (1976); K. Konishi, M. Massoth, A. Ukawa and G. Veneziano, *Phys. Lett. B78*, 243 (1978).

[2] J. Fuster and S. Martí, "Charged Particle Production in the Fragmentation of Quark and Gluon Jets," to appear in the proceedings of the XXXII conference of the European Physics Society, High Energy Physics, Brussels, 27 July- 3 August (1995), hep-ex/9511002, (1996).

[3] P. Abreu et al. (DELPHI Collaboration), CERN-PPE/95-164 "Energy Dependence of the Differences between the Quark and Gluon Jet Fragmentation," to be submitted to *Zeit f. Physik C.*, (1995).

[4] Z. Fodor, "Differences between quark and gluon jets at LEP," *Physics Letters, B263*, p. 305, (1991).

[5] S. Bethke "JADE Results on Quark and Gluon Fragmentation," *Zeit f. Physik C. (Particles and Fields), 29*, p. 175, (1985).

[6] F.H. Heimlich (CRYSTAL BALL Collaboration), "Gluon and Quark Fragmentation in the Upsilon Region," in the Heidelberg 1986, Proceedings, Production and Decay Of Heavy Hadrons, 76-80, (1986).

[7] D. H. Saxon, RAL-86-057 "Quark and Gluon Fragmentation in High-Energy E+ E- Annihilation," based on lectures given at the International School of High Energy Physics, Duilovo-Split, Yugoslavia, Sep 21 - Oct 5, 1986, in Ali, A. (ED.), Soeding, P. (ED.): High Energy Electron-Positron Physics 539-610 and Chilton Rutherford Lab. - RAL-86-057 (86,REC.SEP.) 62p, (1986).

[8] G. Arnison et al. (UA1 Collaboration), "Analysis of the Fragmentation Properties of Quark and Gluon Jets at the CERN SPS P Anti-P Collider," *Nuclear Physics, B276*, p. 253, (1986).

[9] C. J. Maxwell, DTP/85/14 "Investigation of Quark and Gluon Fragmentation" (1986).

[10] R. Waldi (ARGUS Collaboration), "Recent Results from ARGUS on Quark and Gluon Fragmentation in the Upsilon Energy Region," in LUND 1984 Proceedings, Multiparticle Dynamics 808-817 and Heidelberg Univ. IHEP-HD 84-07 (84, REC.SEP.), (1984).

[11] A. Peterson "Further Studies on Quark and Gluon Fragmentation. Recent Results from Jade," DESY 84-082, (1984).

[12] G. C. Moneti HEPSY 6-84 "Gluon Versus Quark Fragmentation," *Lund Multipart.Dyn.*, 1984:782 *QCD161:C49*, (1984).

[13] Paul Hoyer, "Model Independent Analysis of Quark and Gluon Fragmentation," *Physics Letters, B133*, p.108, (1983).

[14] J. William Gary, "On the Multiplicity difference between Quark and Gluon Jets," *Physical Review D 49*, p. 4503, (1994).

[15] E. D. Malaza and B. R. Webber, "Multiplicity Distributions in Quark and Gluon Jets," *Nuclear Physics B 267*, p. 702, (1986).
E. D. Malaza, Z. Phys. C31:143 "Multiplicity Distribution

[16] Yoshihito Iwasaki (SLD Collaboration), "A Measurement of Quark and Gluon Jet Differences at the Z^0 Resonance," SLAC-R-95-460, (1995).

[17] G. Alexander et al. (OPAL Collaboration), "A Direct Observation of Quark-Gluon Jet Differences at LEP," *Physics Letters B265*, p. 462, (1991).

[18] R. Akers (OPAL Collaboration), "A Study of Differences Between Quark and Gluon Jets Using Vertex Tagging of Quark Jets," CERN-PPE/95-075 sub. to Zeit. for Phys. C, (1993).

[19] R. Akers et al. (OPAL Collaboration), "A Model Independent Measurement of Quark and Gluon Jet Properties and Differences," *Zeit. for Phys. C, 68*, p. 179, (1995).

[20] D. Buskulic et al. (ALEPH Collaboration) " Quark and Gluon Jet Properties in Symmetric Three Jet Events," CERN-PPE-95-184, subm. to *Phys. Lett.*, (1995).

[21] Wojtek Bogusz et al. (OPAL Collaboration), Physics Note PN218 "Test of QCD analytic predictions for the mean multiplicity difference between gluon and quark jets", submitted to the 1996 APS Meeting of the Division of Particles and Fields, Minneapolis, MN (1996).

[22] G. Alexander et al. (OPAL Collaboration), "Comparison of b & uds quark jets to gluon jets," *Zeit. for Phys. C 69*, p. 543, (1995).

[23] Y. Kubota *et al*, CLEO Collab., "The CLEO-II detector", Nucl. Instr. Meth. **A320**, 66 (1992).

[24] See, e.g., F. A. Berends and R. Kleiss, Nucl. Phys. **B178**, 141 (1981).

[25] The backgrounds from 'merged' π^0's are, at these energies, negligible due to the good resolution of the CLEO-II detector. See, for example, N. Hancock, 'Determination of the Strong Coupling Constant from Radiative Decays of the $\Upsilon(1S)$ Meson', Ph. D. Thesis, U. of Kansas, 1996 (unpublished), for a fuller discussion of the merged π^0 backgrounds.

[26] Fuster and Martí, for example, predict $R_{chrg} = 0.988 \pm 0.122$ for E_{jet}=10 GeV. They do not extrapolate as low as the energies probed in this measurement, however. [27]

[27] J. Fuster and S. Martí (DELPHI), private communication, and presented at QCD 1996, Montepellier, France.